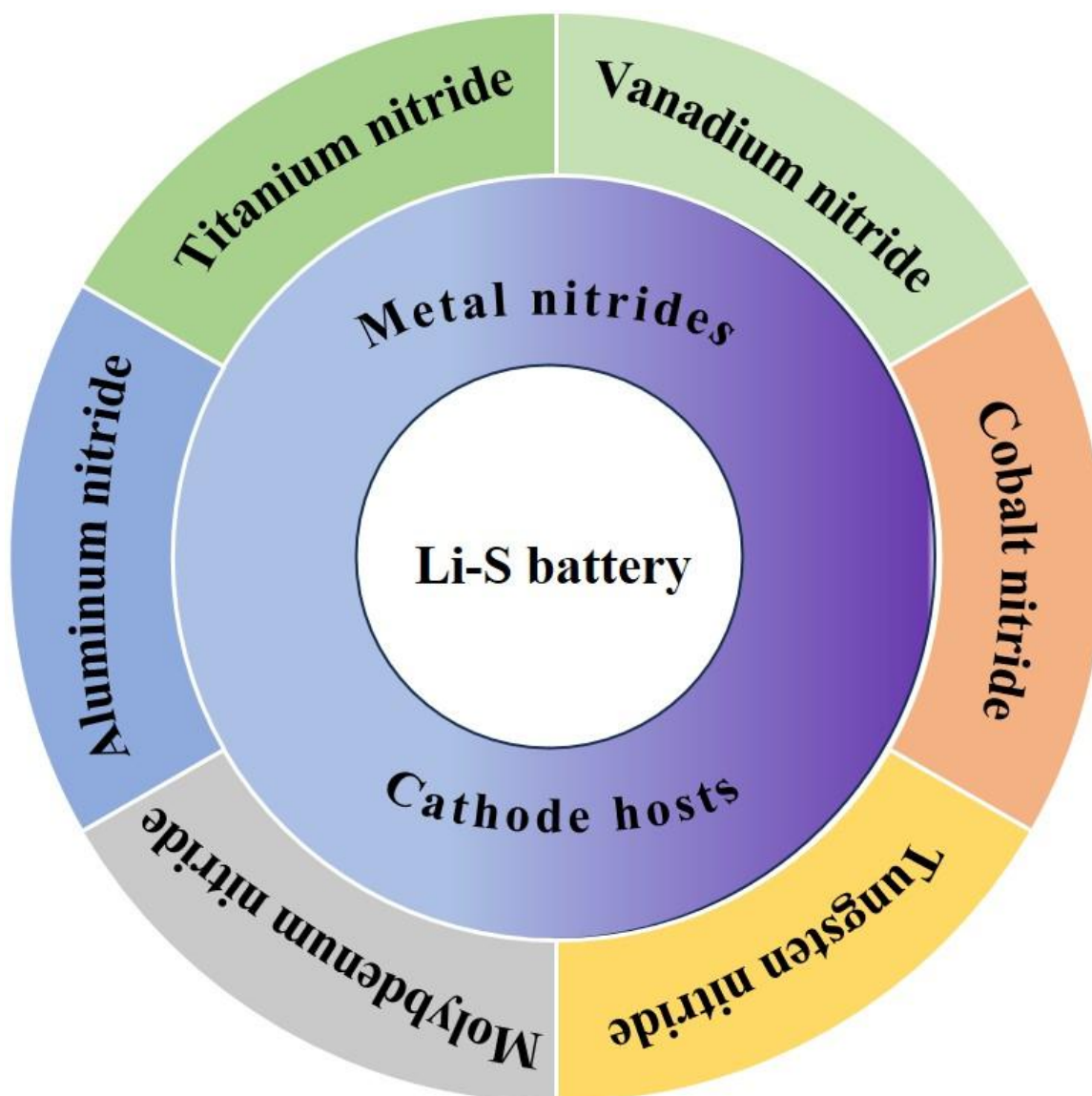


## Metal Nitrides as Cathode hosts for Lithium-Sulfur Batteries

Hai-Ji Xiong <sup>a</sup>, Cheng-wei Zhu <sup>a</sup>, Ding-Rong Deng <sup>a,\*</sup>, Qi-Hui Wu <sup>a,\*</sup>



a Jimei University, College of Marine Equipment and Mechanical Engineering, Key Laboratory of Energy Cleaning Utilization, Development, Cleaning Combustion and Energy Utilization Research Center of Fujian Province, Xiamen Key Laboratory of Marine Corrosion and Smart Protective Materials, Xiamen, Fujian, 361021, China, E-mail: [drdeng@jmu.edu.cn](mailto:drdeng@jmu.edu.cn); [qihui.wu@jmu.edu.cn](mailto:qihui.wu@jmu.edu.cn)

**Keywords:** Lithium-sulfur batteries • Metal nitrides • Host materials

**Abstract:** Lithium-sulfur batteries are considered as one of the potential solutions as integrating renewable energy systems for large-scale energy storage because of the high theoretical energy density ( $2600 \text{ Wh}\cdot\text{kg}^{-1}$ ) and specific capacity ( $1675 \text{ mAh}\cdot\text{g}^{-1}$ ). Due to this face, various strategies have been proposed to overcome the technical barriers, e.g. "shuttle effect", capacity decay, and volumetric change, which impede the successful commercialization of lithium-sulfur batteries. This paper reviews the applications of metal nitrides as the cathode hosts for high-performance lithium-sulfur batteries, summarizes the design strategies of different host materials, discusses the relationship between the properties of metal nitrides and their electrochemical performances. Finally, reasonable suggestions for the design and development of metal nitrides are proposed, along with ideas to promote future breakthroughs. We hope that this review could attract more attention to metal nitrides and their derivatives, and further promote the electrochemical performance of lithium-sulfur batteries.

## 1. Introduction

Over the past decade, lithium-sulfur batteries (LSBs) have made significant progress in various energy storage applications in wide-temperature environments, which have attracted widespread attentions [1-5]. Compared to other secondary battery systems [6-8], LSBs have higher theoretical capacity ( $1675 \text{ mAh}\cdot\text{g}^{-1}$ ) and energy density ( $2600 \text{ Wh}\cdot\text{kg}^{-1}$  and  $2800 \text{ Wh}\cdot\text{L}^{-1}$ ). Moreover, they have advantages such as environmentally friendly reactants and intermediate products within the batteries.

The schematic diagram of a LSB, as shown in Fig 1a, depicts a secondary battery system with sulfur or sulfur-containing compounds as the cathode and lithium metal as the anode [9]. The charge-discharge mechanism of LSBs is rather easy to be understood, but the conversion reactions involved are extremely complex with multiple-electron and multi-step reactions that are not yet fully studied. A widely accepted diagram of the LSBs reaction process, as shown in Fig. 1b, illustrates the overall reactions of the cathode and anode during charge and discharge processes:  $16 \text{ Li}^+ + \text{S}_8 + 16 \text{e}^- \rightarrow 8 \text{ Li}_2\text{S}$  (cathode),  $16 \text{ Li} \rightarrow 16 \text{ Li}^+ + 16 \text{e}^-$  (anode), with the conversion sequence of elemental sulfur generally acknowledged as:  $\text{S}_8 \rightarrow \text{Li}_2\text{S}_8 \rightarrow \text{Li}_2\text{S}_6/\text{Li}_2\text{S}_4 \rightarrow \text{Li}_2\text{S}_2/\text{Li}_2\text{S}$ . Currently, the main obstacles hindering the practical applications of LSBs are threefold: i) poor conductivity of sulfur species; ii) shuttle effect of polysulfides; iii) volume change during charging and discharging [10-12]. Poor conductivity as a battery electrode material is undoubtedly a major issue, with reported conductivities of  $\text{S}_8$  and  $\text{Li}_2\text{S}$  being  $5 \times 10^{-30} \text{ S}\cdot\text{cm}^{-1}$  and  $1 \times 10^{-13} \text{ S}\cdot\text{cm}^{-1}$ , respectively. The poor conductivity of reactants and final products slows down the reaction kinetics inside the

battery, leading to low actual utilization of sulfur [13-15]. Researchers mainly improved the conductivity of the sulfur cathode by employing suitable conductive materials [16-18]. The shuttle effect occurs when lithium ions shuttle back and forth between the cathode and anode during charging and discharging processes. During charging, lithium ions migrate from the cathode to the anode, forming lithium sulfide. Conversely, during discharging, lithium sulfide decomposes, releasing lithium ions, which then shuttle back to the cathode. This repetitive migration of lithium ions between the cathode and anode depletes lithium ions in the electrolyte, reducing the available quantity for charging and discharging, thus lowering the battery's reversible capacity. Additionally, the deposition of sulfides on the electrode surface impedes the transmission of lithium ions, resulting in increase of internal resistance and therefore degraded performance [19]. Moreover, the shuttle effect may cause localized hotspots within the cells, inducing issues such as overheating, leakage, short circuits, and posing safety hazards [20]. The volumetric effect observed in LSBs during charge and discharge processes is due to the significant expansion of the sulfur cathode, exceeding 80%, as it transforms from elemental sulfur to lithium sulfide during cycling [21,22]. This frequent expansion and contraction during charge and discharge causes significant volume changes in the electrode, directly contributing to capacity decay and severe damage to electrode integrity.

Rational design of sulfur composite cathodes can overcome or mitigate the aforementioned issues. Carbon materials used as sulfur hosts in LSBs have garnered considerable attentions. Carbon materials typically exhibit good conductivity, providing excellent electron conduction paths, thereby enhancing the battery's conductivity and charge-discharge performance [16]. Furthermore, the porous structure and high surface area of the material provide more active reaction sites, facilitating the adsorption and immobilization of sulfides, suppressing the shuttle effect, and improving sulfur utilization. The low adsorption capacity of pristine carbonaceous materials for lithium polysulfides leads to severe shuttle effects and rapid capacity decay. Therefore, researchers functionalize carbon materials to enable chemical interactions with the polysulfide species. For example, graphene oxide, materials doped with heteroatoms (N, S, B, O, and P), and conductive polymers have been widely employed [23-27]. Consequently, the concept of "catalytic conversion" was proposed, which envisions the use of appropriate catalysts under rapid battery reaction conditions to facilitate the rapid reactions of adsorbed substances, avoiding the accumulation of long-chain polysulfides, freeing up adsorption sites, promoting the conversion reactions, and further suppressing the shuttle effect as well [28,29]. Metal compounds such as metal oxides, sulfides, and nitrides have been proven to

effectively catalyze the reduction of long-chain polysulfides to short-chain  $\text{Li}_2\text{S}$ , but compared to metal oxides, metal nitrides exhibited higher conductivity and stronger adsorption capacity [30].

The applications of metal nitrides in LSBs offer unique advantages, and greatly enhance the battery performance. Their high conductivity, excellent chemical stability, and tunable porous structure provided an ideal matrix as the composite cathodes for LSBs [31,32]. The chemical bonds between these metal nitride nanomaterials and sulfur effectively restrict the dissolution and shuttle effect of soluble polysulfides, reducing sulfur loss and thereby improving sulfur utilization and the cycling stability of the battery. Therefore, integrating the metal nitrides into the design of LSBs not only demonstrates their technical advantages in nanomaterial fabrication but also opens up new prospects for the commercial applications of LSBs [33,34]. Considering that researchers have extensively summarized the use of metal oxides and metal sulfides in the cathodes of LSBs, this paper reviews the progress of metal nitrides in LSBs systems and briefly outlines their synthesis processes [35-42].

exhibits a cubic crystal structure with a lattice constant of approximately 4.17 Å, resulting in less hindrance to electron motion within the crystal and thereby showing higher conductivity. Furthermore, hexagonal crystal structures of tungsten nitride (WN) and TiN contribute to enhanced electron transport efficiency, thereby improving the energy conversion efficiency and charge-discharge rate of batteries [46,47]. In terms of chemical stability, metal nitrides generally exhibit excellent resistance to chemical corrosion, effectively inhibiting adverse reactions between electrode materials and electrolytes. For example, the chemical inertness and tight crystal structure of VN enable it to effectively prevent the solvent and lithium ion penetration from the electrolyte, thereby prolonging the battery's cycle life [48]. Additionally, WN and TiN, due to their high hardness and stable crystal structure, can withstand mechanical stress and chemical erosion during cycling, maintaining the integrity and performance stability of electrode materials. Therefore, a deep understanding and utilization of metal nitrides as cathode materials for LSBs are of significant importance for enhancing the battery's energy density, cycle stability, and achieving sustainable energy storage.

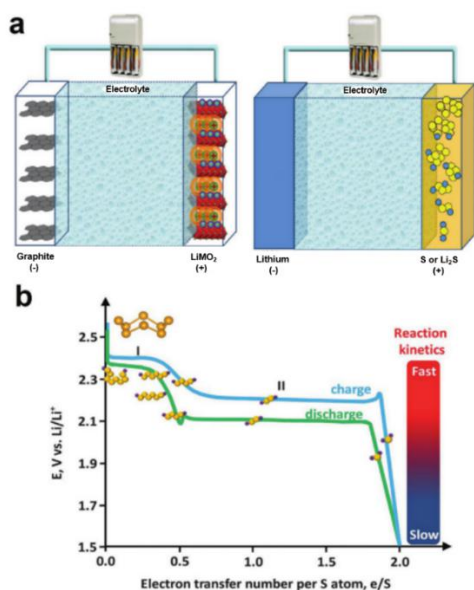


Fig. 1. a) Schematic representation of lithium-ion batteries based on the intercalation reactions (left) and lithium-sulfur battery based on the conversion reaction (right), b) an ideal charge-discharge curve with different sulfur-containing species at different stages, the inset presents the polysulfide shuttling mechanism. Reprinted with permission of Ref. [9], copyright 2017 Wiley-VCH.

## 2. Applications of metal nitrides

Metal nitrides have garnered considerable attentions as the cathode materials for LSBs. Titanium nitride (TiN), vanadium nitride (VN), and cobalt nitride (CoN) have been extensively studied and applied due to their unique crystal structures and chemical properties [43-45]. The electrical conductivity of these materials is mainly influenced by their lattice constants, electron transport pathways, and crystalline defects. For instance, VN

### 2.1. TiN

TiN is an important inorganic compound, which has wide applications in various fields such as aerospace, chemical engineering, and high-temperature and corrosive environments owing to its unique properties [49]. Due to its strong adsorption and good conductivity, it is also commonly used as the host material for LSBs. The electrical conductivity of TiN varies between  $4 \times 10^1$  to  $5.55 \times 10^5 \text{ S}\cdot\text{cm}^{-1}$ , which is comparable to that of metals ( $9 \times 10^6$  to  $6 \times 10^7$ ), facilitating the rapid charge transfer in LSBs [50-52]. Control of the nanostructure of TiN can have a crucial impact on its performance, for instance, high surface area can enhance electrode kinetics and catalyst activity. However, compared to solid sulfur electrodes, the sulfur content in the prepared electrodes is relatively low, thereby limiting the density of the batteries.

Goodenough and colleagues reported a mesoporous TiN as a cathode material for LSBs [53], which significantly improved the utilization of sulfur and optimized the rate performance and cycling stability of the batteries. The mesoporous TiN has a BET specific surface area of  $69.689 \text{ m}^2\cdot\text{g}^{-1}$ , a pore volume of  $0.32 \text{ cm}^3\cdot\text{g}^{-1}$ , and a conductivity of  $46 \text{ S}\cdot\text{cm}^{-1}$  (much higher than ordinary carbon materials). This physical confinement effectively restricts the shuttle of soluble polysulfides. Furthermore, the hydrophilic Ti-O groups of the  $\text{TiO}_2$  passivation layer formed on the surface of TiN can provide polar surfaces that strongly bind with the polysulfides, greatly suppressing the shuttle effect. The initial discharge capacities of TiN-S electrode at 0.5 C current are  $988 \text{ mAh}\cdot\text{g}^{-1}$ . After 500 cycles, the capacity retention rate of TiN-S composite cathode was 65.2%. Although this mesoporous material improves the battery performance, the cycling stability still needs to be enhanced, and the sulfur loading of the cathode sheet also needs to be increased for the true practical application of LSBs.

Considering the strong interaction between TiN and lithium polysulfides, which can suppress the dissolution of polysulfides, our research team synthesized highly conductive hollow mesoporous TiN tubes (as shown in Fig. 2) [54]. The preparation method of these porous tubes involves dissolving  $\text{TiOSO}_4$  in glycerol, ethanol, and diethyl ether to obtain hollow  $\text{TiO}_2$  tubes, and then heating in an ammonia atmosphere to obtain mesoporous TiN tubes. In addition to the high electrical conductivity promoting the reaction kinetics, the large specific surface area of these tubular structures significantly increases the sulfur loading capacity (73.8 wt%). Due to its excellent inherent ability to absorb polysulfides, adding TiN to a  $\text{Li}_2\text{S}_6$  solution results in the  $\text{Li}_2\text{S}_6$  solution turning completely colorless and transparent after 0.5 hours. Furthermore, in cyclic voltammetry (CV) tests, it was found that the reduction peak exhibited a slight negative shift and the oxidation peak showed a significant negative shift, indicating the significant role of TiN in catalyzing the oxidation of short-chain polysulfides to long-chain polysulfides. This is because the nitrogen atoms with lone pairs of electrons can serve as Lewis basic "catalyst" sites, enhancing the adsorption energy of Li in  $\text{Li}_2\text{S}_n$  ( $n = 4-8$ ) and thus promoting the oxidation of LiPSs. Rapid oxidation processes could achieve better charging capacity, thereby improving the Coulombic efficiency of the battery. For example, under a high current density of 1C, the capacity decay rate of the TiN-S electrode from the 3<sup>rd</sup> cycle to the 450<sup>th</sup> cycle is only 0.013%, demonstrating extremely high cycling stability. Furthermore, the TiN-S electrode also exhibited excellent rate performance. At current densities of 0.1 C, 0.2C, 0.5C, 1C, 2C, and 5C, the discharge specific capacities were 1481  $\text{mAh}\cdot\text{g}^{-1}$ , 1338  $\text{mAh}\cdot\text{g}^{-1}$ , 1208  $\text{mAh}\cdot\text{g}^{-1}$ , 1133  $\text{mAh}\cdot\text{g}^{-1}$ , 1110  $\text{mAh}\cdot\text{g}^{-1}$ , and 1026  $\text{mAh}\cdot\text{g}^{-1}$ , respectively. Later on, hollow TiN microspheres were also synthesized as the host for high-performance LSBs [55]. Due to the excellent conductivity ( $8.9\times 10^{-3} \Omega\cdot\text{m}$ ) and hollow porous three-dimensional structure, as well as their adsorption of soluble polysulfides, they could largely improve the performance of LSBs. However, these two TiN porous nanomaterials only emphasized chemical adsorption and promotion of the oxidation reaction in LSBs, however, their promotion of the reduction reaction is not very pronounced.

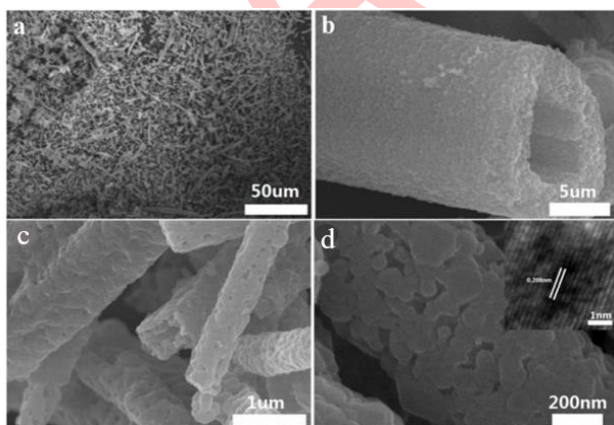


Fig. 2 SEM images of  $\text{TiO}_2$  tubes (a) and (b), and hollow TiN mesoporous tubes (c) and (d) [54].

TiN has a face-centered cubic crystal structure and a relatively small lattice constant, which contribute to enhancing its electron transport efficiency and stability. Current research primarily focuses on analyzing the role and effects of TiN as an electrochemical catalyst in LSBs. This includes TiN influence on the precipitation and dissolution processes of sulfides, as well as its potential in improving the efficiency and cycle stability. However, despite TiN significant advantages such as excellent physicochemical properties and environmental friendliness, its preparation process is relatively complex and costly, which may limit its widespread adoption in commercial applications. For cathode materials in LSBs, the particle size and surface characteristic of TiN plays a crucial role in battery performance. Particle size control during the preparation process may affect its electrochemical performance, which is required further optimization and precise control. Therefore, further research and development of TiN nanomaterials are needed to balance between the preparation cost and performance optimization of TiN, aiming to achieve effective applications in large-scale energy storage systems.

## 2.2. VN

In addition to TiN, VN also has the ability to improve the electrochemical performance of LSBs. Firstly, it exhibits strong adsorption characteristics towards polysulfides, thereby inhibiting their dissolution and consequently suppressing the "shuttle effect". Secondly, at room temperature, VN possesses high electrical conductivity, which is beneficial for enhancing the utilization of sulfur. VN typically exhibits either cubic or hexagonal crystal structures, which facilitate electron transport within the crystal. Furthermore, by designing and optimizing VN's electronic band structure, it can exhibit high electron mobility and conductivity, thereby reducing internal resistance of electrode materials and enhancing the efficiency of electron transport in batteries [56].

Based on these characteristics, Zhan and colleagues designed and prepared a multifunctional sulfur-based material directly grown on the current collector of LSBs [57], which was composed of self-supported porous VN arrays and MOF-derived N-doped carbon nanotubes, with embedded Co nanoparticles named as CC/VN/Co@NCNTs. The schematic diagram of the synthesis process is shown in Fig. 3. CC/VN/Co@NCNTs exhibited strong adsorption capacity to  $\text{Li}_2\text{S}_6$  and accelerated the reaction kinetics of LiPSs. LSBs based on the CC/VN/Co@NCNTs/S electrodes showed good rate performance, with reversible capacities of 1160.4, 950.7, 867.0, 800.0, 739.1, 699.7, and 625.3  $\text{mAh}\cdot\text{g}^{-1}$  at 0.1, 0.2, 0.5, 1, 2, 3, and 5C, respectively. Even after 500 cycles at a current density of 1 C, the discharge specific capacity remained at 499.9  $\text{mAh}\cdot\text{g}^{-1}$ , with the Coulombic efficiency close to 100%, and a capacity decay rate of only 0.063% per cycle, indicating a very low level of degradation.



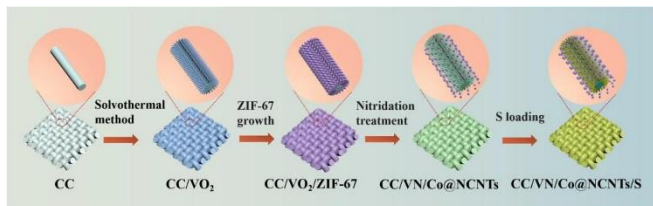


Fig. 3. Schematic illustration for synthesizing the self-standing CC/VN/Co@NCNTs/S cathode electrode. Reprinted with permission of Ref. [57], copyright 2022 Elsevier.

Later, a binder-free VN-based independent was applied as the 3D cathode host for LSBs, which achieved a specific capacity of 1131 mAh g<sup>-1</sup> at 1 C and close to 100% Coulombic efficiency [58]. Wang's research group reported a highly conductive, non-carbon, 3D VN nanowire array as an effective host for both the cathode and anode of LSBs [59]. The nanowires were prepared by hydrothermal reaction of V<sub>2</sub>O<sub>5</sub> powder with H<sub>2</sub>O<sub>2</sub> to obtain V<sub>2</sub>O<sub>5</sub> aerogel, which consists of interwoven ultra-long V<sub>2</sub>O<sub>5</sub> nanowires with an average diameter of 100 nm. After a simple nitriding process, the V<sub>2</sub>O<sub>5</sub> aerogel was transformed into VN aerogel. The VN aerogel nanowires retained the original structure of the V<sub>2</sub>O<sub>5</sub> aerogel with a high aspect ratio. The high conductivity and unique material structure accelerated electron and ion transport.

Current mainstream research on VN as a cathode material for LSBs focused primarily on electrochemical performance optimization, interface engineering and stability studies, as well as nanostructure design and control. However, there has been limited in-depth research on the electrochemical kinetics of VN in LSBs, considering factors such as charge transfer, ion diffusion, and electrode reaction kinetics during charge/discharge processes. Real-time monitoring and analysis of the battery's dynamic behavior are necessary to reveal its electrochemical characteristics and response mechanisms under different charge states, thereby promoting further applications and development.

### 2.3. Cobaltous nitride (Co<sub>4</sub>N)

Co<sub>4</sub>N typically exhibits a hexagonal or cubic crystal system [60]. Co atoms and N atoms are interconnected in a certain arrangement, forming a stable crystal structure. It usually possesses good electrical and thermal conductivity. In terms of chemical stability, Co<sub>4</sub>N can chemically react with other substances under certain conditions, exhibiting a certain degree of chemical activity. Due to its excellent performance, Co<sub>4</sub>N has broad application prospects in various fields [61].

Xiao's research group designed a two-dimensional (2D) metal-organic framework (MOF), where Co<sub>4</sub>N nanoparticles are uniformly embedded in carbon cloth [62]. The preparation method involved using Co(NO<sub>3</sub>)<sub>2</sub>·6H<sub>2</sub>O and 2-methylimidazole as the starting materials, employing a solvent-based method to synthesize 2D sheet-like MOF-Co precursor grown on the surface of carbon cloth. Subsequently, carbonization was conducted at 800°C under Ar protection, resulting in the uniform growth of nano-sized N-doped porous carbon derived from the

Co<sub>4</sub>N-embedded MOF on the carbon cloth fibers with an outer diameter of about 10 μm, forming a unique MOF-Co<sub>4</sub>N composite material. At current densities of 0.1C, 0.5C, and 3C, the reversible specific capacities of MOF-Co<sub>4</sub>N are 1425, 1049, and 729 mAh·g<sup>-1</sup>, respectively. Co<sub>4</sub>N can enhance the cycling performance of LSBs by chemically binding with polysulfides, even after 400 cycles at 1 C, it retains 82.5% of initial capacity. Additionally, its high conductivity and 2D structure provided faster carrier speeds and

more pathways for ion diffusion, thereby promoting the redox reactions. These excellent performances stemmed from its unique structure, which enhanced the affinity for polysulfides and catalyzes redox reactions during discharge and charge processes, thus improving rate capability and cycling performance. The potential difference between the discharge and charge platforms of MOF-Co<sub>4</sub>N is only 0.329 V, which is smaller than that of MOF-Co (0.379 V) and MOF-C, indicating lower polarization in LSBs based on the MOF-Co<sub>4</sub>N cathode host. The negative shift of the reduction peak in the CV curve suggests that Co<sub>4</sub>N can optimize the reversibility of LSBs and catalyze the conversion of soluble polysulfides to final products. X-ray photoelectron spectroscopy (XPS) analysis of the fully discharged state of MOF-Co<sub>4</sub>N and MOF-Co<sub>4</sub>N/S electrodes confirmed the chemical adsorption properties of MOF-Co<sub>4</sub>N and its high affinity for lithium polysulfides. Specifically, it could be observed that compared with the Co-N peak in the previously reported pure Co<sub>4</sub>N structure, the Co-N peak was slightly shifted to higher binding energy [63] due to the transfer of electrons from Co to the N-doped carbon matrix. After discharge, a new peak appeared at 782.8 eV, confirming the chemical interaction between Co and lithium polysulfides.

For LSBs, achieving high sulfur utilization and cycling stability is the key factor. Our group reported mesoporous Co<sub>4</sub>N spheres [64] by dissolving Co(CH<sub>3</sub>COO)<sub>2</sub> and PVP in ethylene glycol. After calcination, Co<sub>3</sub>O<sub>4</sub> spheres were obtained, which were then heated in an ammonia atmosphere at 400°C for four hours to gain mesoporous Co<sub>4</sub>N spheres with surface area and pore volume of 48.4 m<sup>2</sup>·g<sup>-1</sup> and 0.237 cm<sup>3</sup>·g<sup>-1</sup>. These mesoporous spheres provided abundant pore structures for sulfur storage, offer more adsorption and catalytic sites for polysulfides, thereby significantly enhanced the specific capacity and cycling stability of LSBs (Fig. 4a). Mesoporous Co<sub>4</sub>N spheres exhibited high affinity for polysulfides and served as dual-functional catalysts for the sulfur redox process, providing a discharge specific capacity close to the theoretical capacity (1675 mAh·g<sup>-1</sup>) reaching 1659 mAh·g<sup>-1</sup>. Experimental data showed that they not only possessed excellent rate performance and cycling stability, the low-valence Co elements but also played a major role in the catalytic process. The low polarization of LSBs based on Co<sub>4</sub>N mesoporous spheres is attributed to their stronger adsorption capacity for LiPSs, which effectively suppressed the "shuttle effect." Fig. 4b shows the excellent rate performance and high specific capacity of Co<sub>4</sub>N/S. Moreover, LSBs based on Co<sub>4</sub>N maintained excellent cycling stability even at high current densities. After 1000 cycles, the capacities still remain at 761 mAh·g<sup>-1</sup>, with Coulombic efficiency close to 100% (Fig. 4c).

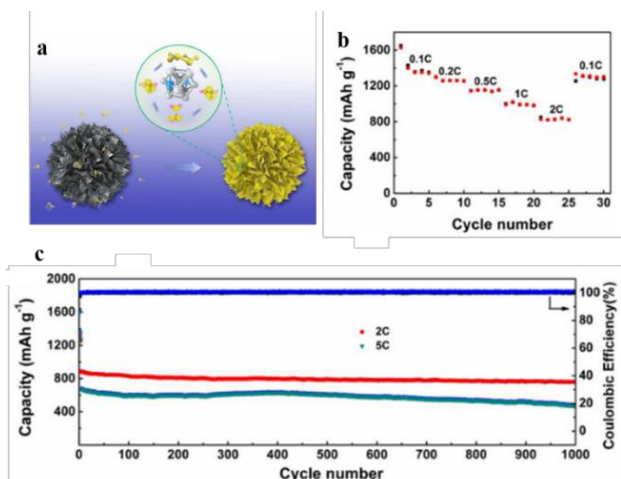


Fig. 4. (a) Schematic illustration of Co<sub>4</sub>N sphere and its interaction with LiPSs during discharge/charge process of the lithium-sulfur battery. (b) Rate capability of Co<sub>4</sub>N/S at different current rates. (c) The charge and discharge capacity versus cycle number at current densities of 2 C and 5 C [64].

Due to its specific crystal structure and electronic band structure design, Co<sub>4</sub>N exhibits excellent electrical conductivity, however, the electronic structure modulation and electron transport mechanism of Co<sub>4</sub>N remain unclear. A deeper understanding of electronic structure modulation strategies for Co<sub>4</sub>N, such as doping, surface modification, or structural engineering to optimize its electronic levels and electron transport performance, is thus necessary. Combining electrochemical techniques and theoretical calculations to explore the microscopic mechanisms of electron transport when Co<sub>4</sub>N is used as an electrode material can facilitate the rational cathode design.

## 2.4. Aluminum nitride (AlN)

AlN is an important III-V group nitride semiconductor material. It possesses excellent thermal conductivity, electrical insulation, and mechanical properties [65], which also can serve as an electrode substrate material for LSBs. It would enhance the electrode's conductivity and structural stability, thereby improving the battery's cycling and rate performance [66,67]. Wu and colleagues reported a composite material of AlN@N-doped carbon nanosheets (AlN@NCNs) used as the cathode host in LSBs [68]. The AlN nanoparticles loaded with 3D crosslinked N-doped carbon nanosheets were prepared through a simple liquid-phase reaction and nitridation processes. Specifically, a mixture of trisodium citrate dihydrate (C<sub>6</sub>H<sub>5</sub>Na<sub>3</sub>O<sub>7</sub>·2H<sub>2</sub>O) and melamine (C<sub>3</sub>H<sub>6</sub>N<sub>6</sub>) in a mass ratio of 10:15 was uniformly mixed. After calcination at 750°C for 2.5 hours, black N-doped carbon Ns were obtained. Subsequently, the NCNs and nonahydrate aluminum nitrate (Al(NO<sub>3</sub>)<sub>3</sub>·9H<sub>2</sub>O) were dispersed in deionized water. After complete solvent evaporation, the sample was calcined at 1000°C in nitrogen atmosphere for 2 hours to obtain AlN@NCNs. In the 3D crosslinked network structure, the CNs are crosslinked, which

facilitates the transfer of electrons between cathodes (Fig. 5). Additionally, the 3D crosslinked network structure has a large specific surface area and abundant porous structure, which can enhance the contact area of the electrolyte, shorten the transfer path of electrons/ions, and thus improve the cathode conductivity. The AlN@NCNs/S composite material was prepared by melt diffusion method by mixing AlN@NCNs and S powders in a mass ratio of 1:2.5 with the S content approximately 70.7%. The resistance of the AlN@NCNs/S cathode has superior conductivity, and the electron and ion transfer rates. Because pyridinic nitrogen, pyrrolic nitrogen, and graphitic nitrogen can generate additional defects inside carbon, which is conducive to the chemical adsorption of LiPSs. Coupled with the excellent conductivity of AlN@NCNs, LSBs based on AlN@NCNs/S electrodes exhibit good rate performance and cycling stability. At 0.2 A·g<sup>-1</sup>, the initial discharge capacity of AlN@NCNs/S was 1297.2 mAh·g<sup>-1</sup>, and after 300 cycles, the discharge capacity of the AlN@NCNs/S cathode was 459.1 mAh·g<sup>-1</sup>, with a capacity decay rate of 0.21% per cycle. The discharge capacities at 0.1, 0.2, 0.5, 1.0, and 2.0 A·g<sup>-1</sup> were 934.6, 824.8, 700.8, 560.4, and 342.6 mAh·g<sup>-1</sup>, respectively.

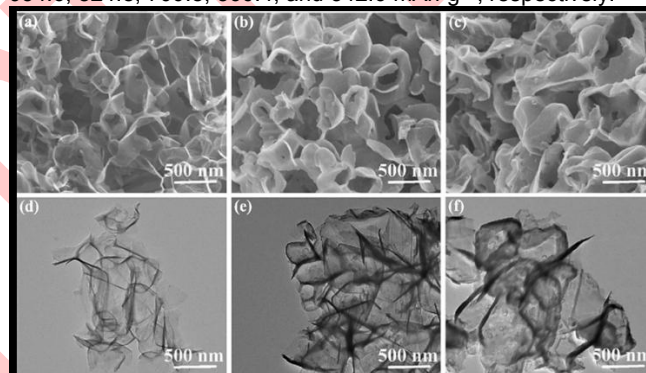


Fig. 5. SEM images of (a) NCN, (b) AlN@NCNs, and (c) AlN@NCNs/S. TEM images of (d) NCNs, (e) AlN@NCNs, and (f) AlN@NCNs/S. Reprinted with permission of Ref. [68], copyright 2023 Elsevier.

The crystal structure of AlN is hexagonal (wurtzite structure), characterized by highly symmetrical and closely packed atomic arrangements. This structure facilitates rapid heat transfer within the lattice, thereby enhancing the material's overall thermal conductivity, which helps maintain stable operating temperatures in batteries and reduces the risk of thermal runaway. However, the preparation process of AlN is relatively complex, especially for large-area and high-efficiency preparation techniques, which require further optimization and development. Additionally, despite its chemical stability, the interface engineering and compatibility of AlN with sulfides need further research and optimization to enhance its efficiency and cycle stability as a cathode material in LSBs.

## 2.5. Molybdenum nitrides (MoN/Mo<sub>2</sub>N)

MoN/Mo<sub>2</sub>N are considered as interstitial alloys with excellent conductivity and decent hardness. High electrical conductivity can accelerate the electron transfer in LSB systems, promoting

internal redox reactions [69]. Additionally, due to the difference in electronegativity between the metal Mo and non-metal N, Molybdenum nitrides exhibit polarity, which can suppress the "shuttle effect". Therefore, the successful preparation of porous MoN/Mo<sub>2</sub>N with a high surface area as the sulfur host is an effective way to promote the interaction with polysulfides and consequently improve the performance of LSBs [70].

Wang and colleagues reported a mesoporous Mo<sub>2</sub>N material using a mesoporous silica template based on nitridation process, which was applied as the sulfur host for LSBs [71]. The mesoporous Mo<sub>2</sub>N has a surface area of up to 121 m<sup>2</sup>·g<sup>-1</sup>, a pore size of 8.6 nm, and an electrical conductivity of 1×10<sup>5</sup> S·m<sup>-1</sup>. The high electrical conductivity contributes to electron transfer, improving the utilization of sulfur. The mesoporous Mo<sub>2</sub>N provided nanoscale spaces that could be used to accommodate and physically confine sulfur. In addition, Mo<sub>2</sub>N provided more polar surfaces, closely interacting with the sulfur species, effectively binding LiPSs, thereby suppressing their "shuttle effect". LSBs based on the mesoporous Mo<sub>2</sub>N exhibited good cycling performance, with the capacity still maintaining 77% of its initial capacity of 995 mAh·g<sup>-1</sup> after 200 cycles. The charge-discharge curves of LSBs exhibited a stable discharge platform after 200 cycles, further demonstrating its excellent cycling stability. The excellent electrochemical performance of the mesoporous Mo<sub>2</sub>N/S cathode can be attributed to the synergistic effect of its mesoporous structure, electrical conductivity, and polarity, thereby suppressing the "shuttle effect," promoting the oxidation-reduction reactions of polysulfides, and optimizing battery performance.

The utilization of sulfur hosts with strong immobilization and catalytic effects on soluble polysulfides is crucial for the development of advanced LSBs. On this basis, Liu's research group prepared MoN nanorods using a one-pot ammoniation strategy using (NH<sub>4</sub>)<sub>6</sub>Mo<sub>7</sub>O<sub>24</sub>·4H<sub>2</sub>O, NaCl as the precursors and polyvinylpyrrolidone as the template [72]. The MoN nanorods have a porous network with a size of 3-5 nm, a specific surface area of 60 m<sup>2</sup>·g<sup>-1</sup>, and a pore volume of 0.462 cm<sup>3</sup>·g<sup>-1</sup> (Fig. 6). When used as the positive electrode material for LSBs, the prepared MoN/S composite electrode provided an initial discharge capacity of up to 1315 mAh·g<sup>-1</sup> with a high sulfur loading of 3.1 mg·cm<sup>-2</sup>, and maintained a reversible capacity of 902 mAh·g<sup>-1</sup> after 350 cycles.

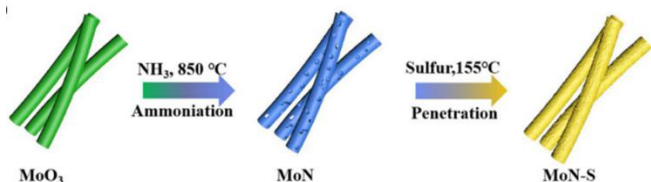


Fig. 6. Schematic synthesis procedure of MoN and MoN-S. Reprinted with permission of Ref. [72], copyright 2020 Elsevier.

Excellent electrical conductivity and good electrocatalytic activity make MoN/Mo<sub>2</sub>N promising candidates for cathode materials in LSBs. However, achieving high-quality and high-purity molybdenum nitrides typically requires complex

preparation processes and expensive raw materials, resulting in relatively high production costs.

## 2.6. WN

WN is typically gray-black powders, exhibiting good electrical conductivity and thermal conductivity with a cubic crystal structure, which is similar to other transition metal nitrides such as titanium nitride (TiN) [73,74]. As a conductive additive, WN can improve the conductivity of electrodes, facilitate the electron transfer of lithium ions and sulfides, thereby enhancing the rate capability and electrochemical performance of batteries, thus improving the cycling stability and capacity retention of batteries [75].

Ma and colleagues designed a 3D porous layered WN nanoblock to confine Li<sub>2</sub>S<sub>6</sub> and Li<sub>2</sub>S<sub>4</sub>, thereby preventing the soluble polysulfides from dissolving into the electrolyte and avoiding irreversible loss of active materials caused by the shuttle effect [76]. Based on the density functional theory (DFT) calculations, the binding energies between various Li<sub>x</sub>S<sub>n</sub> polysulfides and the crystal plane surface (WN (200)) of WN were calculated. The binding energy of WN (200) to Li<sub>2</sub>S<sub>8</sub> is 4.01 eV, and as the length of soluble polysulfide molecules decreases, the calculated binding energy of WN (200) to Li<sub>2</sub>S<sub>4</sub> gradually decreases to 1.44 eV. In further partial density of states (PDOS) calculations, almost all PDOS peaks between the S 2p and W 3d orbitals show significant overlap, while there is only a small peak overlap between the Li 1s and N 2p orbitals in the energy range of -5 to -4 eV, suggesting that this strong adsorption effect is due to the formation of S-W bonds rather than Li-N bonds. With the suppression of shuttle effects, the battery shows higher Coulombic efficiency. The charge-specific capacity of the composite cathode at a current density of 0.5 C is 1090 mAh·g<sup>-1</sup>. After 20 cycles at current densities of 0.5 C, 1 C, 2 C, and 5 C, the charge capacity recovers to 950 mAh·g<sup>-1</sup> when the current density is reduced to 0.5 C. After 500 cycles at a current density of 2 C, the capacity remained at 358 mAh·g<sup>-1</sup>, with a decay rate of 0.13% per cycle, and the Coulombic efficiency remains stable close to 100%.

Mosavati's group reported the applications of WN as the cathode host for LSBs [77]. The preparation method involved dissolving ammonium tungstate in HCl. The resulting yellow tungsten oxide was then heated at 700 °C in a tube furnace under NH<sub>3</sub> atmosphere, yielding WN nanosheets with an average size of 290 nm and a specific surface area of 16.7 m<sup>2</sup>·g<sup>-1</sup> (Fig. 7). In cyclic voltammetry (CV) tests of LSBs using 0.2 M Li<sub>2</sub>S<sub>8</sub> catholyte, which exhibited larger current density and smaller polarization.

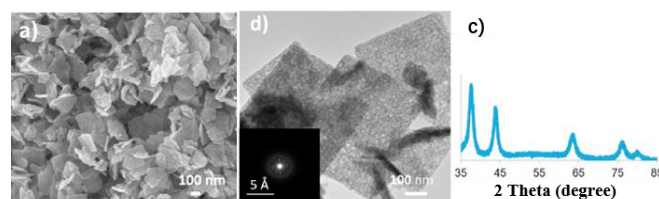




Fig. 7. (a) SEM image of WN, (b) TEM images and SAED patterns of WN, (c) Powder XRD pattern of WN. Reprinted with permission of Ref. [77], copyright 2017 Elsevier.

The electronic structure of W enables WN to exhibit high electron mobility and conductivity, facilitating rapid electron transfer in electrode materials. Additionally, WN demonstrates high chemical inertness, showing low reactivity towards solvents and lithium ions in electrolytes, which helps reduce adverse chemical reactions and maintain battery stability. The preparation process of WN is relatively mature and its structure and performance can be tuned by controlling preparation conditions and methods. This controllability allows researchers to optimize the crystal structure, surface characteristics, and electrochemical active sites of WN, further enhancing its performance as a battery cathode material. However, there are still critical research aspects that have been overlooked, including long-term stability, dynamic response, interface modulation, high-temperature stability, and validation in practical application environments. Future research needs to focus on these aspects to comprehensively understand and optimize the application potential of WN in LSBs.

### 3. General guidelines for the design of cathode hosts for LSBs and conclusions

Metal nitrides have been employed as typical polar host materials in LSBs to effectively encapsulate sulfur and anchor polysulfides (Table 1). However, there exist thousands of metal nitrides with

vastly different nanostructures and surfaces, utilized in the electrochemical conversion of LSB systems. Thus, how to design appropriate metal nitrides in LSB systems? In complex electrochemical reactions, the interaction between metal nitrides and polysulfides is a crucial factor. For instance,  $\text{Co}_4\text{N}$  and  $\text{TiN}$ , the most commonly used metal nitride materials in LSBs, were subjected to XPS and Raman spectroscopy tests after

interacting with the polysulfides, serving as effective tools to probe whether the host materials possess adsorption capabilities towards polysulfides. Furthermore, visualizing the host material before and after contacting  $\text{Li}_2\text{S}_6$  serves as a vivid approach to confirm the interaction between metal nitrides and polysulfides [94,95]. Moreover, density functional theory (DFT) has been widely employed to investigate the complex interactions between polysulfides and host materials. By theoretical calculations, the adsorption energy barriers between the host materials and  $\text{Li}_2\text{S}_x$  ( $1 \leq x \leq 8$ ) are obtained, facilitating the assessment of catalysts' influence on sulfur adsorption, desorption, and electrochemical reactions in LSBs, thus guiding material design and performance optimization [96,97]. On the other hand, the electrical conductivity of materials is also an extremely important factor [98]. In complex multi-step conversion reactions, poor conductivity can slow down the reaction kinetics, whereas good conductivity ensures effective electron transfer, significantly affecting the extent to which sulfur is ultimately converted to  $\text{Li}_2\text{S}$ . Moreover, if the substrate material can act as an electrocatalyst to lower the overpotential of the lithium polysulfide redox reaction, it will further accelerate the reaction kinetics. Therefore, an ideal polar substrate should have good conductivity and exhibit some catalytic activity towards the conversion of lithium polysulfides, which will facilitate the liquid-to-liquid transition of polysulfides and the liquid-to-solid nucleation/growth of  $\text{Li}_2\text{S}$ . Since most metal nitrides exhibit good conductivity but relatively low surface area, considering the small surface area may affect the number of adsorption sites, which could influence the adsorption efficiency of polysulfides. Therefore, if metal nitrides are intended to be used as host materials, it is advisable to select those with strong affinity for polysulfides, high electrochemical activity, and excellent surface diffusion performance to ensure rapid reaction kinetics after the formation of liquid-phase intermediates. Additionally, the nanostructure plays a crucial role in the performance of materials [99]. For instance, the specific surface area, pore distribution, and pore volume of metal nitrides depend on their nanostructure, which also regulates the adsorption capacity for polysulfides.

Table 1. Different metal nitrides employed in cathodes of lithium-sulfur batteries

Polar host material	Synthesis method	Morphology	Sulfur loading & (sulfur content in cathode by weight) $[\text{mg} \cdot \text{cm}^{-2}]$ & $[\%]$	Voltage window (vs. $\text{Li}^+$ ) $[\text{V}]$	Electrochemical performance (initial capacity $\{\text{mAh} \cdot \text{g}^{-1}\}$ and cycles) & decay Rate claimed (per cycle)	Sulfur infiltration method	Ref.
TiN	Solid-solid phase separation method	Mesoporous sphere	0.6816	1.6-2.8	988(65.2% after 500 cycle) at C/2 & (N/A)	Melt-diffusion	[53]



TiN-VN@CNFs	electrospinning method	Multichannel structure of the fibers	5.6	1.7-2.8	1388 at C/10(1110 after 100 cycles at C/5) & 0.051% at 1 C	Melt-diffusion	[54]
CNTs@TiN-TiO <sub>2</sub>	atomic layer deposition	Deposition of TiN layer on the CNT surface	15	1.5-3	1431(1330 after 350 cycles) at C/5 & 0.0056% at 1 C, 0.031% at 2 C	Li <sub>2</sub> S <sub>6</sub> and electrolyte (lithium/dissolved polysulfide systems)	[80]
TiN	Hydrothermal method	Hollow and porous nanostructure	70 wt%	1.7-2.7	692 at 5 C (740 after 400 cycles at 1 C) & 0.006% at 1 C	Melt-diffusion	[82]
TiN	Hydrothermal and calcined	Hollow porous tubes	73.8 wt%	1.7-2.7	1026 at C/5(above 840 after 450 cycles at C/2)	Melt-diffusion	[83]
CNT@TiN	Mild solvothermal method and a nitriding process	Nanoparticles	1	N/A	1175(734 after 100 cycles) at C/5 & 0.19%	Melt-diffusion	[84]
TMN	Taku-san chemical synthesis method	2D arrays of few-nanometer nanocrystals	5.1	N/A	912.8(796.5% after 1000 cycles at 1 C) & 0.013%	Melt-diffusion	[86]
TiN	Heating method	Nanostructures	7	1.5-3	1524(358 after 100 cycles) at C/10 & N/A	S <sub>8</sub> Li <sub>2</sub> S and electrolyte	[87]
TiN	Hydrothermal and Heating method	Hollow TiN microspheres	60 wt%	1.8-2.8	1218(623.3 after 300 cycles) & N/A	Melt-diffusion	[88]
VN	Hydrothermal method	Pea shape nanoparticles,	8	1.5-3	573(N/A)	Lithium/dissolved polysulfide systems	[77]
VN/G	Hydrothermal and annealing method	3D interconnected network	3&(N/A)	1.7-2.8	1471(above 99.5% after 100 cycle) at C/2 & 0.15%	Li <sub>2</sub> S <sub>6</sub> and electrolyte (lithium/dissolved polysulfide systems)	[72]
VN	Hydrothermal and facile nitridation treatment	Aerogel nanowires	4 & (40 wt%)	1.8-2.8	1121(836 after 400 cycles) & 0.06%	Melt-diffusion	[85]
VN	molten salt template method	Porous structure	70 wt%	1.7-2.8	1050(75% after 100 cycles) at C/5 & 0.059%	Melt-diffusion	[92]
VN	calcination, washing and polyaniline-coating	Porous rod-like structure	70 wt%	1.6-2.8	1007(735 after 150 cycles) at 0.5 A/g & N/A	Melt-diffusion	[93]

p-Fe <sub>2</sub> N/n-VN PNCf	soft template and electrospinning technology	Heterostructure	6.5(71 wt%)	N/A	1358.2(93% after 300 cycles) at C/10 & N/A	Melt-diffusion	[90]
VN/M/NC	molten salt Template method	Small and uniformly dispersed VN particles	70 wt%	1.7-2.8	798(81.5% after 500 cycles) at 1C & 0.036%	Melt-diffusion	[91]
MVN@C NWs	Hydrothermal AND nitridation	Mesopores structure	2.7(57.2 wt%)	1.6-3	1040 at 1 C (735 after 200 cycles at 2 C) & N/A	Soaking with S/CS <sub>2</sub> and Melt- diffusion	[93]
MOF-Co <sub>4</sub> N	facile solvent method	2D nitrogen- doped carbon structure	1(N/A)	1.7-2.8	1425(≈82.5 after 400 cycle) at 1 C & (N/A)	Li <sub>2</sub> S <sub>6</sub> and electrolyte (lithium/dissolved polysulfide systems)	[62]
Co <sub>4</sub> N	Hydrothermal method	Mesoporous sphere	72.3 wt%	1.7-2.7	1659(above 94% after 100 cycle) at C/2 & 0.01%	Melt-diffusion	[79]
CuCoN <sub>0.6</sub> /NC	electrospinning and nitridation method	Necklace-like	2.72	1.7-2.8	1218(85.2% after 100 cycles) at C/10 & 0.076%	Li <sub>2</sub> S <sub>6</sub> and electrolyte (lithium/dissolved polysulfide systems)	[89]
Mo <sub>2</sub> N	soft templating approach	Mesoporous sphere	1.1	1.7-2.8	995(91.9% after 100 cycle) at C/2 & 0.081%	Melt-diffusion	[71]
MoN	one-pot ammoniation strategy	3D network structure	3.1	1.7-2.8	1315(990 after 350 cycles) at 1 C & 0.062%	Melt-diffusion and annealing	[72]
MoN@CMK- 5	Hydrothermal method	bimodal pore system	70 wt%	1.7-2.8	1582 at 0.1 C (475.8 after 1000 cycles) at 5 C & 0.027%	Melt-diffusion	[81]
WN	Hydrothermal method	Face-centered cubic (fcc) structure	8	1.5-3	697(700 after 100 cycles)	Lithium/dissolved polysulfide systems	[85]
Mo <sub>2</sub> N	Hydrothermal method	Mesoporous nano rod shaped porous	8	1.5-3	264(N/A)	Lithium/dissolved polysulfide systems	[77]
WN	self-templating hydrothermal reaction	3D porous hierarchical WN nanobolcks	0.92(52 wt%)	1.7-2.8	N/A (358 after 500 cycles at 2 C)	Melt-diffusion	[77]
AlN@NCNs	Heating, drying, washing, precipitation, drying	Cross-linked thin nanosheets	70.7 wt%	1.6-2.8	1297(459.1 after 300 cycles) at 0.2 A/g & N/A	Melt-diffusion	[59]

reactions leading to irreversible capacity loss; ii) electrical conductivity of materials or composite materials; iii) catalytic capability to promote the mutual conversion between lithium polysulfides (Li<sub>2</sub>S<sub>x</sub> (4≤x≤8)) and lithium disulfide. This can enhance the charging/discharging rates, improving cycling stability, suppressing dendrite growth, and increasing energy density; iv) surface area, 3D morphology, and exposure of active sites in nanoscale structures of materials. For the practical

application of LSBs, it is necessary to consider various factors comprehensively to provide an integrated solution. Not only emerging issues such as new characterization methods and theoretical predictions for the future development of LSBs need to be addressed but also some fundamental issues, such as low areal sulfur loading, excessive electrolyte usage, and low volumetric energy density, need to be gradually overcome. Taking the example of sulfur loading in cathodes predominantly consisting of nanoscale metal nitrides, which typically falls within the range of 0.5 to 2 mg·cm<sup>-2</sup>, there is still a long way to go before LSBs can be truly practical [100]. And some metal nitrides often interact with sulfides, which may lead to undesirable chemical reactions or the formation of unstable compounds, affecting the performance of the battery. For example, TiN in LSBs may react with sulfides to form titanium sulfides or other titanium-sulfur compounds [101], which could impact the electrochemical performance and stability of the battery. When selecting, it is preferable to choose metal nitrides with good chemical compatibility with sulfides, or to apply coatings or modifications to the surface of the metal nitrides to prevent adverse reactions. Additionally, it is worth noting that the synthesis routes of some metal nitrides are relatively more complex compared to other inorganic materials and may involve the use of strong acids, which could potentially cause environmental damage [102], thereby limiting their large-scale application in LSBs. Under these circumstances, exploring low-cost and easily synthesizable materials will facilitate further applications of metal nitrides in LSBs.

## 29 Declaration of Competing Interest

The authors declare that they have no known competing financial interests or personal relationships.

## 32 Acknowledgements

This work was financially supported by NSFC (22379051, 22172062). Supported by Fund of Xiamen Key Laboratory of Marine Corrosion and Smart Protective Materials.

## 36 References

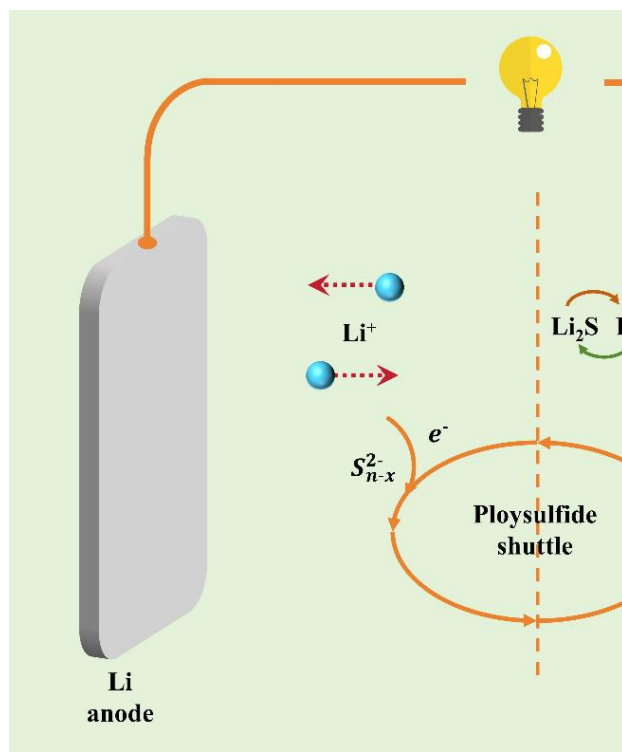
- [1] Guo Y, Niu Q, Pei F, Wang Q, Zhang Y, Du L Y, Zhang Y, Zhang Y S, Zhang Y Y, Fan L, Zhang Q Y, Yuan L X, Huang Y X. Interface Engineering Toward Stable Lithium-Sulfur Batteries[J]. *Energy Environ. Sci.*, 2024, 17(4): 1330-1367.
- [2] Deng D R, Cui X Y, Wu Q H, Zheng M S, Dong Q F. In-situ synthesis TiO<sub>2</sub> nanosheets@rGO for ultrafast sodium ion storage at both room and low temperatures[J]. *J Alloys Compd.*, 2020, 835: 155413.
- [3] Xiong H J, Luo Y L, Deng D R, Zhu C W, Song J X, Weng J C, Wu Q H, Fan X H, Li G F, Zeng Y, Li Y. In-situ synthesis Fe<sub>3</sub>C@C/rGO as matrix for high performance lithium-sulfur batteries at room and low temperatures[J]. *J Colloid Interface Sci.*, 2024, 668: 448-458.
- [4] You Y, Zhang F J, Yu H Z, Li Q, Liu Q Z. Fe<sub>2</sub>O<sub>3</sub>-Decorated hollow CNT as efficient cathode coatings for high-performance lithium-sulfur batteries[J]. *Mater. Today Commun.*, 2024, 38: 108479.
- [5] Song Y W, Shen L, Yao N, Feng S, Cheng Q, Ma J, Zhang Q, Chen X, Li B Q. Anion-Involved Solvation Structure of Lithium Polysulfides in Lithium-Sulfur Batteries[J]. *Angew. Chem. Int. Ed.*, 2024, 63(19): e202400343.
- [6] Salehi H, Maroufi S, Mofarah S S, Nekouei R K, Sahajwalla V. Recovery of rare earth metals from Ni-MH batteries: A comprehensive review[J]. *Renew. Sust. Energ. Rev.*, 2023, 178: 113248.
- [7] Menz F, Bauer M, Böse O, Pausch M, Danzer M A. Investigating the Thermal Runaway Behaviour of Fresh and Aged Large Prismatic Lithium-Ion Cells in Overttemperature Experiments[J]. *Batteries*, 2023, 9(3): 159-159.
- [8] Deng D R, Xiong H J, Luo Y L, Yu K M, Weng J C, Li G F, Wu Q H, Lei J, Zheng M S. Accelerating the Rate Determining Steps of Sulfur Conversion Reaction for Lithium-Sulfur Batteries Working at an Ultrawide Temperature Range[J]. *Adv. Mater.*, 2024: 2406135.
- [9] Li X, Huang J Q, Zhang Q, Mai Q. Nanostructured Metal Oxides and Sulfides for Lithium-Sulfur Batteries[J]. *Adv. Mater.*, 2017, 29(20): 1601759.
- [10] Wild M, O'Neill L, Zhang T, Purkayastha R, Minton G, Marinescu M, Offer G J. Lithium sulfur batteries, a mechanistic review[J]. *Energy Environ. Sci.*, 2015, 8(12): 3477-3494.
- [11] Gicha B B, Tufa L T, Nwaji N, Hu X, Lee J. Advances in All-Solid-State Lithium-Sulfur Batteries for Commercialization[J]. *Nanomicro Lett*, 2024, 16(1): 172.
- [12] Zheng S, Khan N, Worku B E, Wang B. Review and prospect on low-temperature lithium-sulfur battery[J]. *Chem. Eng.*, 2024, 484: 149610.
- [13] Liu Y, Wu F, Hu Z, Zhang F, Wang K, Li L, Chen R. Regulating Sulfur Redox Kinetics by Coupling Photocatalysis for High-Performance Photo Assisted Lithium-Sulfur Batteries[J]. *Angew. Chem. Int. Ed.*, 2024, 63(25): e202402624.
- [14] Deng D R, Wu Q H, Li Y. Electronic structure of graphene/MoO<sub>3</sub>/CuPc interfaces[J]. *Mater. Res. Express.*, 2019, 6(12): 126315.
- [15] Song Y Z, Song L X, Wang M L, Cai W L. Chemical vapor deposition making better lithium-sulfur batteries[J]. *Sci. Bull.*, 2024, 16: S2095-9273.
- [16] Ji X L, Lee K T, Nazar L F. A highly ordered nanostructured carbon-sulphur cathode for lithium-sulphur batteries[J]. *Nat. Mater.*, 2009, 8(6): 500-506.
- [17] Jayaprakash N, Shen J, Moganty S S. Porous hollow carbon@sulfur composites for high-power lithium-sulfur batteries[J]. *Angew. Chem. Int. Ed.*, 2011, 123(26): 6026-6030.
- [18] Guo J, Xu Y, Wang C. Sulfur-Impregnated Disordered Carbon Nanotubes Cathode for Lithium-Sulfur Batteries[J]. *Nano Lett.*, 2011, 11(10): 4288-4294.
- [19] Sadd M, De Angelis S, Colding-Jorgensen S. Visualization of Dissolution-Precipitation Processes in Lithium-Sulfur Batteries[J]. *Adv. Energy Mater.*, 2022, 12(10): 2103126.
- [20] Zhu K P, Li L H, Xue P, Pu J, Wu L Y, Guo G D, Wang R, Zhang Y, Peng H S, Hong G, Zhang Q, Yao Y G. "Three - in - one" strategy: Heat regulation and conversion enhancement of a multifunctional separator for safer lithium-sulfur batteries[J]. *Carbon Energy*, 2023, 5(11): e352.
- [21] Wang D W, Zeng Q, Zhou G. Carbon-sulfur composites for Li-S batteries: status and prospects[J]. *J. Mater. Chem. A*, 2013, 1(33): 9382-9394.
- [22] Fei B, Zhang C, Cai D. Hierarchical Nanoreactor with Multiple Adsorption and Catalytic Sites for Robust Lithium-Sulfur Batteries[J]. *ACS nano*, 2021, 15(4): 6849-6860.
- [23] Hu X C, Zhu X S, Ran Z S, Liu S H, Zhang Y Y, Wang H, Wei W. Conductive Polymer-Based Interlayers in Restraining the Polysulfide Shuttle of Lithium-Sulfur Batteries[J]. *Molecules*, 2024, 29(5): 1164.
- [24] Fei Y, Li G. Unveiling the Pivotal Parameters for Advancing High Energy Density in Lithium-Sulfur Batteries: A Comprehensive Review[J]. *Adv. Funct. Mater.*, 2024, 34(21): 2312550.
- [25] Song Z H, Jiang W Y, Li B R, Qu Y P, Mao R Y, Jian X G, Hu F Y. Advanced Polymers in Cathodes and Electrolytes for Lithium-Sulfur Batteries: Progress and Prospects[J]. *Small*, 2024, 20(19): 2308550.
- [26] Chen J J, Fu Y Q, Guo J C. Development of Electrolytes under Lean Condition in Lithium-Sulfur Batteries[J]. *Adv. Mater.*, 2024: 2401263.
- [27] Deng D R, Xue F, Bai C D, Lei J, Yuan R M, Sen Zheng M, Dong Q F. Enhanced adsorptions to polysulfides on graphene-supported BN nanosheets with excellent Li-S battery performance in a wide temperature range[J]. *ACS Nano*, 2018, 12(11): 11120-11129.



- [28] Deng D R, Cui X Y, Fan X X, Zheng J Q, Fan X H, Wu Q H, Zheng M S, Dong Q F. Integration of adsorption and catalytic active sites in cobalt iron oxide nanorods for an excellent performance Li-S battery with a wide temperature range[J]. *Sustain. Energy. Fuels.*, 2021, 5(17): 4284-4288.
- [29] Borchardt L, Oschatz M, Kaskel S. Carbon materials for lithium sulfur batteries-ten critical questions[J]. *Chem. Eur. J.*, 2016, 22(22): 7324-7351.
- [30] Dasarathan S, Sung J H, Ali M, Lee Y J, Choi H Y, Park J W, Kim D. Effect of phosphorus-modified TiN mesoporous MXene interlayer as a polysulfide electrocatalyst in Li-S battery[J]. *Electrochem commun.*, 2024, 160: 107679.
- [31] Yin R J, Wan L, Xue H T, Wei C D, Liu M W, Zhao W, Tang F L. First-principles study of the catalytic performance of sulfur cathode host Co<sub>3</sub>Mo<sub>3</sub>N<sub>4</sub>[J]. *Comput. Mater. Sci.*, 2024, 238: 112946.
- [32] Lu S, Cai L C, Wang J Q, Ying H J, Han Z K, Han W Q, Chen Z P. 2D Ultrathin Titanium Nitride Nanosheets as Separator Coatings for Li-S Batteries[J]. *Small*, 2024, 20(27): 2307784.
- [33] Liu R Q, He L L, Liu Y R, Wu J Y, Zhu W F, Xie K, Liu W X, Lin X J, Shi L, Wang S, Feng X M, Ma Y W. Multistep C/VN frameworks as highly-efficient sulfur host for high-performance lithium-sulfur batteries[J]. *Mater. Chem. Phys.*, 2024, 315: 129045.
- [34] Liu J T, Yu L H, Ran Q W, Chen X A, Wang X Y, He X D, Jin H L, Chen T, Chen J S, Guo D Y, Wang S. Regulating Electron Filling and Orbital Occupancy of Anti - Bonding States of Transition Metal Nitride Heterojunction for High Areal Capacity Lithium-Sulfur Full Batteries[J]. *Small*, 2024: 2311750.
- [35] Kadam S A, Jose L M, George N S, Sreehari S, Nayana D A, Van Pham D, Kadam K P, Aravind A, Ma Y R. Recent progress in transition metal nitride electrodes for supercapacitor, water splitting, and battery applications[J]. *J Alloys Compd.*, 2023, 976: 173083.
- [36] Wang T, Dong Q, Wang F Z, Xu R, Tong C, Su D, Shao M H, Li C P, Wei Z D. Functionless cobalt toward functional cobalt nitride: Catalytic sulfur carrier for lithium-sulfur pouch batteries[J]. *Mater.*, 2024, 7(3): P1035-1053.
- [37] Jin L N, Chen J Y, Fu Z H, Qian X Y, Cheng J, Hao Q Y, Zhang K. ZIF-8/ZIF-67 derived ZnS@Co-NC hollow core-shell composite and its application in lithium-sulfur battery[J]. *SM&T*, 2023, 35(6): e00571.
- [38] Zhang P, Yue L L, Liang Q Y, Gao H, Yan Q, Wang L. A Review of Transition Metal Compounds as Functional Separators for Lithium-Sulfur Batteries[J]. *ChemistrySelect*, 2023, 8(1): e202203352.
- [39] Li J, Zhang X, Zhang Z Y, Li Y R, Zhu L L. Preparation of LDHs-derived Co-Ni<sub>3</sub>N heterostructure modified porous carbon nanofibers as advanced interlayers for lithium-sulfur batteries[J]. *J Alloys Compd.*, 2024, 971: 72731.
- [40] Mori R. Cathode materials for lithium-sulfur battery: a review[J]. *J Solid State Electrochem.*, 2023, 27(4): 813-839.
- [41] Zhang X D, Zhao M C, Cai D P, Zhang C Q, Chen Q D, Zhan H B. Separator modified by ternary iron molybdenum nitride and nitrogen-doped carbon composite enabling efficient polysulfide conversion for lithium-sulfur batteries[J]. *J. Alloys Compd.*, 2023, 967: 171633.
- [42] Han Z, Son S, Kim K, Geng M Z, Yang H Q. Manganese nitride/oxide heterostructure interlayer derived from triazolate metal-organic framework for stable Li-S batteries[J]. *Chem. Eng. J.*, 2024, 481: 148389.
- [43] Wang Y K, Zhang R F, Pang Y C, Chen X, Lang J X, Xu J J, Xiao C H, Li H L, Xi K, Ding S J. Carbon@titanium nitride dual shell nanospheres as multi-functional hosts for lithium sulfur batteries[J]. *Energy Stor. Mater.*, 2019, 16: 228-235.
- [44] Ma L B, Wang Y R, Wang Z W, Wang J L, Cheng Y W, Wu J X, Peng B, Xu J, Zhang W, Jin Z. Wide-Temperature Operation of Lithium-Sulfur Batteries Enabled by Multi-Branched Vanadium Nitride Electrocatalyst[J]. *ACS Nano.*, 2023, 17(12): 11527-11536.
- [45] Yang J, Li S Q, Wu G Z, Bao J W, Xu S, Gu C P, Lv J J, Huang J R, Joo S W. Preparation of polyaniline-coated cobalt nitride nanoflowers as sulfur host for advanced lithium-sulfur battery[J]. *J. Alloys Compd.*, 2024, 981: 173701-173701.
- [46] Deng D J, Zhang H H, Wu J C, Tang X, Ling M, Dong S H, Xu L, Li H A, Li H M. Electronic structure and spin state regulation of vanadium nitride via a sulfur doping strategy toward flexible zinc-air batteries[J]. *J. Energy Chem.*, 2024, 89: 239-249.
- [47] Sekiya T, Yamada T, Yamane H. Synthesis of faceted crystal grains of titanium nitride using titanium oxides, boron nitride, and sodium[J]. *J. Ceram. Soc. JAPAN*, 2020, 128(7): 364-367.
- [48] Xu W C, Pan X X, Meng X, Zhang Z H, Peng H R, Liu J, Li G C. A conductive sulfur-hosting material involving ultrafine vanadium nitride nanoparticles for high-performance lithium-sulfur battery[J]. *Electrochim. Acta*, 2020, 331: 135287-135287.
- [49] Xie D, Wang X T, Wei L J, Zhang R, Ganesan R, Matthews D T A, Leng Y X. Atomic configuration, electronic structure, and work of adhesion of TiN (111)/B2 - NiTi (110) and TiN (111)/B19' - NiTi (010) interfaces: Insights from first - principles simulations[J]. *Surf Interface Anal.*, 2023, 55(1): 41-51.
- [50] Morales H M, Vieyra H, Sanchez D A, Fletes E M, Odlyzko M, Lodge T P, Padilla-Gainza V, Alcoutlabi M, Parsons J G. Synthesis and Characterization of Titanium Nitride-Carbon Composites and Their Use in Lithium-Ion Batteries[J]. *Nanomaterials*, 2024, 14(7): 624.
- [51] Avasarala B, Haldar P. Electrochemical oxidation behavior of titanium nitride based electrocatalysts under PEM fuel cell conditions[J]. *Electrochim. Acta*, 2010, 55(28): 9024-9034.
- [52] Lu X H, Wang G M, Zhai T, Yu M H, Xie S L, Ling Y C, Liang C L, Tong Y X, Li Y. Stabilized TiN nanowire arrays for high-performance and flexible supercapacitors[J]. *Nano Lett.*, 2012, 12(10): 5376-5381.
- [53] Cui Z M, Zu C X, Zhou W D, Manthiram A, Goodenough J B. Mesoporous Titanium Nitride-Enabled Highly Stable Lithium-Sulfur Batteries[J]. *Adv. Mater.*, 2016, 28(32): 6926-6931.
- [54] Deng D R, An T H, Li Y J, Wu Q H, Zheng M S, Dong Q F. Hollow porous titanium nitride tubes as a cathode electrode for extremely stable Li-S batteries[J]. *J. Mater. Chem. A*, 2016, 4(41): 16184-16190.
- [55] Deng D R, Wu Q H. Hollow TiN Microspheres Synthesized by a Template - Free Method as a Matrix for High Performance Li-S Battery[J]. *ChemistrySelect*, 2020, 5(28): 8735-8739.
- [56] Zhao J, Zhao Y Y, Yue W C, Li X, Gao N, Zhang Y J, Hu C Q. V<sub>2</sub>O<sub>5</sub>/VN catalysts decorated free-standing multifunctional interlayer for high-performance Li-S battery[J]. *Chem. Eng. J.*, 2022, 441: 136082.
- [57] Cai D P, Zhuang Y X, Fei B, Zhang C Q, Wang Y G, Chen Q D, Zhan H B. Self-supported VN arrays coupled with N-doped carbon nanotubes embedded with Co nanoparticles as a multifunctional sulfur host for lithium-sulfur batteries[J]. *Chem. Eng. J.*, 2022, 430(P3): 132931.
- [58] Wang L, Sun C Y, Ji S, Linkov V, Wang H. Highly - Dispersed Vanadium Nitride Supported on Porous Nitrogen - Doped Carbon Material as a High-Performance Cathode for Lithium-Sulfur Batteries[J]. *ChemistrySelect*, 2022, 7(45): e202202879.
- [59] Sun C Y, Ji S, Ma X G, Wang H, Wang X Y, Linkov V, Wang R F. Using sp<sup>2</sup> N atom anchoring effect to prepare ultrafine vanadium nitride particles on porous nitrogen-doped carbon as cathode for lithium-sulfur battery[J]. *J. Colloid Interface Sci.*, 2022, 623: 306-317.
- [60] Azouaoui A, Benzakour N, Hourmatallah A, Bouslykhane K. Study of structural, electronic, magnetic, elastic, and thermodynamic properties of Co<sub>3</sub>N antiperovskite by first principles and Monte Carlo simulation[J]. *Phys. Status Solidi*, 2021, 258(2): 2000339.
- [61] Jia H N, Fan J H, Su P, Guo T T, Liu M C. Cobalt Nitride Nanoparticles Encapsulated in N - Doped Carbon Nanotubes Modified Separator of Li-S Battery Achieving the Synergistic Effect of Restriction Adsorption Catalysis of Polysulfides[J]. *Small*, 2024, 20(26): 2311343.
- [62] Xiao K K, Wang J, Chen Z, Qian Y H, Liu Z, Zhang L L, Chen X H, Liu J L, Fan X F, Shen Z X. Improving polysulfides adsorption and redox kinetics by the Co<sub>3</sub>N nanoparticle/N - doped carbon composites for lithium-sulfur batteries[J]. *Small*, 2019, 15(25): 1901454.
- [63] Li Z Q, Li C X, Ge X L, Ma J Y, Zhang Z W, Li Q, Wang C X, Yin L W. Reduced graphene oxide wrapped MOFs-derived cobalt-doped porous carbon polyhedrons as sulfur immobilizers as cathodes for high performance lithium-sulfur batteries[J]. *Nano Energy*, 2016, 23: 15-26.
- [64] Deng D R, Xue F, Jia Y J, Ye J C, Bai C D, Zheng M S, Dong Q F. Co<sub>4</sub>N nanosheet assembled mesoporous sphere as a matrix for ultrahigh sulfur content lithium-sulfur batteries[J]. *ACS nano*, 2017, 11(6): 6031-6039.
- [65] Wang Z, Wang X, Tong Y G, Wang Y P. Impact of structure and flow-path on in situ synthesis of AlN: Dynamic microstructural evolution of Al-AlN-Si materials[J]. *Sci. China Mater.*, 2018, 61(7): 948-960.

- [66] Jackson N, Mathewson A. Enhancing the piezoelectric properties of flexible hybrid AlN materials using semi-crystalline parylene[J]. *Smart Mater Struct*, 2017, 26(4): 045005.
- [67] Hou X R, Li L, Wei S C, Li J D, Wu F C. Two-dimension Al<sub>2</sub>O<sub>3</sub>-AlN heterogeneous nanosheets as bifunctional host materials for kinetics-accelerated and dendrite-free lithium-sulfur batteries[J]. *Electrochim. Acta*, 2023, 464: 142887.
- [68] Yang J, Wu G Z, Sun A J, Gu C P, Cao Y X, Joo S W, Huang J R. AlN nanoparticles anchored on cross-linked N-doped carbon nanosheets as sulfur hosts for lithium-sulfur battery[J]. *J. Electroanal. Chem.*, 2023, 951: 117930.
- [69] Abdelkader H S, Rabahi A, Benaissa M, Benabadji M K. Theoretical investigation of structural and mechanical stability of Mo<sub>2</sub>N[J]. *Solid State Commun*, 2020, 314-315: 113919.
- [70] Yang J L, Cai D Q, Lin Q W, Wang X Y, Fang Z Q, Huang L, Wang Z J, Hao X G, Zhao S X, Li J, Cao G Z, Lv W. Regulating the Li<sub>2</sub>S deposition by grain boundaries in metal nitrides for stable lithium-sulfur batteries[J]. *Nano Energy*, 2022, 91: 106669.
- [71] Jiang G S, Xu F, Yang S H, Wu J P, Wei B Q, Wang H Q. Mesoporous, conductive molybdenum nitride as efficient sulfur hosts for high-performance lithium-sulfur batteries[J]. *J. Power Sources*, 2018, 395: 77-84.
- [72] Liu H D, Chen Z L, Man H, Yang S P, Song Y, Fang F, Chen R C, Sun D L. Template-guided synthesis of porous MoN microrod as an effective sulfur host for high-performance lithium-sulfur batteries[J]. *J. Alloys Compd.*, 2020, 842: 155764.
- [73] Xing W D, Zhang Y, Meng F Y, Wang C C, Tao Q, Zhu P W, Zhu J, Yu R. Structure stabilization effect of configuration entropy in cubic WN[J]. *Phys. Chem. Chem. Phys.*, 2018, 20(46): 29243-29248.
- [74] Yan N F, Cui H M, You S Y, Shi J S, Weng Y Q, Liu Y W. Tungsten nitride nanotubes as sulfur host material for high performance Li-S batteries[J]. *Inorg Chem Commun*, 2022, 140: 109458.
- [75] Liu H, Shen H, Li R, Liu S, Turak A, Yang M. Tungsten-Nitride-Coated Carbon Nanospheres as a Sulfur Host for High-Performance Lithium-Sulfur Batteries[J]. *ChemElectroChem*, 2019, 6(7): 2074-2079.
- [76] Huang Z D, Fang Y W, Yang M T, Yang J K, Wang Y Z, Wu Z, Du Q C, Masese T, Liu R Q, Yang X S, Qian C H, Jin S W, Ma Y W. Sulfur in mesoporous tungsten nitride foam blocks: a rational lithium polysulfide confinement experimental design strategy augmented by theoretical predictions[J]. *ACS Appl. Mater. Interfaces*, 2019, 11(22): 20013-20021.
- [77] Mosavati N, Salley S O, Ng K Y S. Characterization and electrochemical activities of nanostructured transition metal nitrides as cathode materials for lithium sulfur batteries[J]. *J. Power Sources*, 2017, 340: 210-216.
- [78] Sun Z H, Zhang J Q, Yin L C, Hu G J, Fang R P, Cheng H M, Li F. Conductive porous vanadium nitride/graphene composite as chemical anchor of polysulfides for lithium-sulfur batteries[J]. *Nat. Commun.*, 2017, 8: 14627.
- [79] D R Deng, Xue F, Jia Y J, Ye J C, Bai C D, Zheng M S, Dong Q F. Co<sub>2</sub>N nanosheet assembled mesoporous sphere as a matrix for ultrahigh sulfur content lithium-sulfur batteries[J]. *ACS nano*, 2017, 11(6): 6031-6039.
- [80] Zhang H, Ono L K, Tong G Q, Liu Y Q, Qi Y B. Long-life lithium-sulfur batteries with high areal capacity based on coaxial CNTs@TiN-TiO<sub>2</sub> sponge[J]. *Nat. Commun.*, 2021, 12(1): 4738.
- [81] Liu Z H, Lian R Q, Wu Z R, Li Y J, Lai X Y, Yang S, Ma X, Wei Y J, Yan X. Ordered Dual-Channel carbon embedded with molybdenum nitride catalytically induced High-Performance Lithium-Sulfur battery[J]. *Chem. Eng. J.*, 2022, 431(P2): 134163-134163.
- [82] Deng D R, Wu Q H. Hollow TiN Microspheres Synthesized by a Template-Free Method as a Matrix for High Performance Li-S Battery[J]. *ChemistrySelect*, 2020, 5(28): 8735-8739.
- [83] Yao Y, Wang H Y, Yang H, Zeng S F, Xu R, Liu F F, Shi P C, Feng Y Z, Wang K, Yang W J, Wu X J, Luo W, Yu Y. A dual-functional conductive framework embedded with TiN-VN heterostructures for highly efficient polysulfide and lithium regulation toward stable Li-S full batteries[J]. *Adv. Mater.*, 2020, 32(6): 1905658.
- [84] Wang Y K, Zhang R F, Sun Z H, Wu H, Lu S Y, Wang J N, Yu W, Liu J M, Gao G X, Ding S J. Spontaneously Formed Mott-Schottky Electrocatalyst for Lithium-Sulfur Batteries[J]. *Adv. Mater., Interfaces* 2020, 7(22): 1902092.
- [85] He J R, Manthiram A. Long-life, high-rate lithium-sulfur cells with a carbon-free VN host as an efficient polysulfide adsorbent and lithium dendrite inhibitor[J]. *Adv. Energy Mater.*, 2020, 10(3): 1903241.
- [86] Xiao X, Wang H, Bao W Z, Urbankowski P, Yang L, Yang Y, Maleski K, Cu L F, Billinge S J L, Wang G X, Gogotsi Y. Two-dimensional arrays of transition metal nitride nanocrystals[J]. *Adv. Mater.*, 2019, 31(33): 1902393.
- [87] Mosavati N, Chitturi V R, Salley S O, Ng K Y S. Nanostructured titanium nitride as a novel cathode for high performance lithium/dissolved polysulfide batteries[J]. *J. Power Sources*, 2016, 321: 87-93.
- [88] Chen L, Yang W W, Zhang H, Liu J G, Zhou Y. Self-templated preparation of hollow mesoporous TiN microspheres as sulfur host materials for advanced lithium-sulfur batteries[J]. *J. Mater. Sci.*, 2018, 53(14): 10363-10371.
- [89] Liu D, Wang Z C, Guo Z C, Tian Y, Wang C. Electrospun CuCoN<sub>0.6</sub> coating necklace-like N-doped carbon nanofibers for high performance lithium-sulfur batteries[J]. *J. Colloid Interface Sci.*, 2023, 645: 705-714.
- [90] Liu J T, Yu L H, Ran Q W, Chen X A, Wang X Y, He X D, Jin H L, Chen T, Chen J S, Guo D Y, Wang S. Regulating Electron Filling and Orbital Occupancy of Anti-Bonding States of Transition Metal Nitride Heterojunction for High Areal Capacity Lithium-Sulfur Full Batteries[J]. *Small*, 2024: 2311750.
- [91] Sun C Y, Ji S, Ma X G, Wang H, Wang X Y, Linkov V, Wang R F. Using sp<sup>2</sup> N atom anchoring effect to prepare ultrafine vanadium nitride particles on porous nitrogen-doped carbon as cathode for lithium-sulfur battery[J]. *J. Colloid Interface Sci.*, 2022, 623: 306-317.
- [92] Lv J J, Ren H B, Cheng Z Y, Joo S W, Huang J R. Polyaniline-coated porous vanadium nitride microrods for enhanced performance of a lithium-sulfur battery[J]. *Molecules*, 2023, 28(4): 1823.
- [93] Li X X, Ding K, Gao B, Li Q W, Li Y Y, Fu J J, Zhang X M, Chu P K, Huo K F. Freestanding carbon encapsulated mesoporous vanadium nitride nanowires enable highly stable sulfur cathodes for lithium-sulfur batteries[J]. *Nano Energy*, 2017, 40: 655-662.
- [94] Pang Q, Kundu D, Nazar L F. A graphene-like metallic cathode host for long-life and high-loading lithium-sulfur batteries[J]. *Mater. Horizons*, 2016, 3(2): 130-136.
- [95] Hart C J, Cuisinier M, Liang X, et al. Rational design of sulphur host materials for Li-S batteries: correlating lithium polysulphide adsorptivity and self-discharge capacity loss[J]. *ChemComm*, 2015, 51(12): 2308-2311.
- [96] Song J, Xu T, Gordin M L, et al. Nitrogen-doped mesoporous carbon promoted chemical adsorption of sulfur and fabrication of high-areal-capacity sulfur cathode with exceptional cycling stability for lithium-sulfur batteries[J]. *Adv. Funct. Mater.*, 2014, 24(9): 1243-1250.
- [97] Hou T Z, Peng H J, Huang J Q, et al. The formation of strong-couple interactions between nitrogen-doped graphene and sulfur/lithium (poly) sulfides in lithium-sulfur batteries[J]. *2D Mater.*, 2015, 2(1): 014011.
- [98] Peng H J, Zhang G, Chen X, et al. Enhanced electrochemical kinetics on conductive polar mediators for lithium-sulfur batteries[J]. *Angew. Chem. Int. Ed.*, 2016, 55(42): 12990-12995.
- [99] Wang H, Zhang Q, Yao H, et al. High electrochemical selectivity of edge versus terrace sites in two-dimensional layered MoS<sub>2</sub> materials[J]. *Nano Lett.*, 2014, 14(12): 7138-7144.
- [100] Zhao M, Li B Q, Peng H J, et al. Challenges and opportunities towards practical lithium-sulfur batteries under lean electrolyte conditions[J]. *Angew. Chem. Int. Ed.*, 2020, 132: 2-20.
- [101] Kamali A R, Fray D J. Tin-based materials as advanced anode materials for lithium ion batteries: a review[J]. *Rev. Adv. Mater. Sci.*, 2011, 27(1): 14-24.
- [102] Yang Z G, Xu H M, Shuai T Y, et al. Recent progress in the synthesis of transition metal nitride catalysts and their applications in electrocatalysis[J]. *Nanoscale*, 2023, 15(28): 11777-11800.

## Entry for the Table of Contents





# 金属氮化物作为锂硫电池阴极硫骨架材料的研究

熊海基<sup>a</sup>, 朱成威<sup>a</sup>, 邓丁榕<sup>a\*</sup>, 吴启辉<sup>a\*</sup>

(<sup>a</sup>. 集美大学海洋装备与机械工程学院, 福建 厦门 361021)

**摘要:** 由于锂硫电池高理论能量密度 ( $2600 \text{ Wh}\cdot\text{kg}^{-1}$ ) 和比容量 ( $1675 \text{ mAh}\cdot\text{g}^{-1}$ ), 被认为是集成可再生能源系统用于大规模能量存储的潜在解决方案之一。但是由于“穿梭效应”、容量衰减和体积变化等障碍阻碍了锂硫电池的成功商业化。现阶段已提出各种策略以克服技术障碍, 本文综述了不同金属氮化物作为高性能锂硫电池阴极宿主材料的应用, 总结了不同宿主材料的设计策略, 讨论了金属氮化物性质与其电化学性能之间的关系, 最后, 提出了对金属氮化物设计和发展的合理建议, 以及促进未来突破的想法。我们希望本文能够引起更多关于金属氮化物及其衍生物的关注, 并进一步促进锂硫电池的电化学性能。

**关键词:** 锂硫电池; 金属氮化物; 正极材料